AIP Journal of Applied Physics

A comparative ab initio study of superconductivity in the body centered tetragonal YC2 and LaC2

H. M. Tütüncü and G. P. Srivastava

Citation: Journal of Applied Physics **117**, 153902 (2015); doi: 10.1063/1.4918309

View online: http://dx.doi.org/10.1063/1.4918309

View Table of Contents: http://scitation.aip.org/content/aip/journal/jap/117/15?ver=pdfcov

Published by the AIP Publishing

A comparative *ab initio* study of superconductivity in the body centered tetragonal YC_2 and LaC_2

H. M. Tütüncü[1,2] and G. P. Srivastava[3]
[1]*Sakarya Üniversitesi, Fen-Edebiyat Fakültesi, Fizik Bölümü, 54187 Adapazarı, Turkey*
[2]*Sakarya Üniversitesi, Biyomedikal, Manyetik ve Yarıiletken Malzemeler Araştırma Merkezi (BIMAYAM), 54187 Adapazarı, Turkey*
[3]*School of Physics, University of Exeter, Stocker Road, Exeter EX4 4QL, United Kingdom*

(Received 22 December 2014; accepted 5 April 2015; published online 15 April 2015)

Ab initio studies of the electronic band structure and phonon dispersion relations, using the planewave pseudopotential method and the density functional theory, have been made for the superconducting materials YC_2 and LaC_2. Differences in the phonon spectrum and density of states both in the acoustical and optical ranges between these materials are investigated and discussed. By integrating the Eliashberg spectral function $\alpha^2F(\omega)$, the average electron-phonon coupling parameter is found to be $\lambda = 0.55$ for YC_2 and 0.54 for LaC_2, indicating these to be weak-coupling BCS superconductors. It is established that about 60% of λ is contributed by acoustic phonons in both materials. Using a reasonable value of $\mu^* = 0.13$ for the effective Coulomb repulsion parameter, the superconducting critical temperature T_c is found to be 3.81 K for YC_2 and 2.44 K for LaC_2, in good agreement with values reported from experimental measurements. © *2015 AIP Publishing LLC*.
[http://dx.doi.org/10.1063/1.4918309]

I. INTRODUCTION

Carbides of the transition metals have attracted interest for decades due to their unique physical and chemical properties. They show ultra-hardness and high melting points as well as metallic conductivity. These properties can be linked to their three different types of bonding characteristics: ionic, covalent, and metallic.[1–3] Moreover, some mono-carbides[4–6] show superconductivity with transition temperatures up to 25 K. In addition to monocarbides such as NbC, TaC, and CrC, dicarbides such as YC_2 and LaC_2 are also superconductors. In contrast to the wealth of experimental and theoretical works[6] presented in recent years on the structural, elastic, electronic, vibrational, and superconducting properties of NbC, TaC, and CrC, there have been limited experimental and theoretical works on these properties of YC_2 and LaC_2. On the experimental side, Gülden and co-workers[7] characterized the superconducting state of YC_2, $Y_{1-x}Th_xC_2$, and $Y_{1-x}Ca_xC_2$ $(0 < x \leq 0.3)$ from magnetization and specific measurements. Their work shows that YC_2 is a superconductor with the transition temperature (T_C) of 4.02 K, slightly larger than a previously reported experimental value of 3.88.[8] In their experimental work, Gülden *et al.* also presented the electronic structure and electronic density of states (eDOS) for YC_2 using the tight-binding linear muffin-tin orbital atomic-sphere approximation (TB-LMTO-ASA) method.[7] The full-potential linear muffin-tin method and the generalized gradient approximation (FLMTO-GGA) have been also used to examine the electronic properties of YC_2.[9] In this theoretical work, the experimental lattice parameters from Ref. 7 were used as input data. First-principles calculations based on density functional theory (DFT)[10] are also used to investigate the stability, elastic constants, hardness, Debye temperature, and mechanical anisotropy properties of YC binary compounds. In this theoretical work,[10] the local density approximation (LDA) is used for the exchange correction energy. Recently, Babizhetskyy and co-workers[11] have synthesized polycrystalline samples of superconducting LaC_2 and investigated these by x-ray and neutron powder diffraction techniques, magnetic susceptibility, and heat capacity measurements. Their work indicated that LaC_2 is a superconductor with the transition temperature (T_C) slightly below 1.80 K, in good accordance with a previous experimental value of 1.60 K.[12] In this experimental work, the electronic structure of LaC_2 was also calculated by employing the self-consistent TB-LMTO method. These authors also compared the electronic structure of LaC_2 with that of YC_2 and showed that the topology of the electronic band structure of the two materials is quite similar.

Phonons play the role of bringing about the coupling between electrons to form Cooper pairs, the main building blocks of the BCS theory of superconductivity. However, no systematic theoretical attempt has been made to make a comparative study of the phonon properties of YC_2 and LaC_2. This work is aimed at making *ab initio* calculations of the structural, electronic, and phonon properties of YC_2 and LaC_2 in the body-centered tetragonal CaC_2 structure. Using our electronic and phonon results, the Eliashberg function $\alpha^2F(\omega)$ and the electron-phonon mass enhancement parameter λ for these materials have been calculated. Finally, the superconducting parameters for both materials are presented and compared with each other, and an explanation is forwarded for observed differences.

II. THEORY

All calculations were performed by the first-principles calculations based on the density functional theory implemented in the QUANTUM ESPRESSO code.[13] For the exchange–correlation function, we used the GGA of

Perdew–Burke–Ernzerhof (PBE), known as PBE–GGA.[14] Vanderbilt ultrasoft pseudo potentials[15] are used to describe the electron-ion interaction. The electronic structure calculations are made by solving the Kohn-Sham equation,[16] and minimizing the total energy with respect to relaxation of electrons, ions, and unit cell parameters in a self-consistent way. The Monkhorst–Pack scheme[17] is chosen for **k** point sampling in the Brillouin zone (BZ). The k points are set at $24 \times 24 \times 24$ for electronic calculations. The kinetic energy cutoff is taken to be 60 Ry for the plane waves while the augmentation charges are expanded up to 240 Ry. Integration up to the Fermi surface has been made using the smearing technique with the smearing parameter $\sigma = 0.02$ Ry.

The lattice dynamics of YC_2 and LaC_2 has been studied in the framework of the harmonic approximation to the force constants and using the linear response method.[13] The Kohn-Sham equations are solved at the $8 \times 8 \times 8$ **k**-points mesh for our phonon calculations. The dynamical matrices have been computed on a $4 \times 4 \times 4$ **q**-points mesh, and a Fourier interpolation has been used to obtain phonon frequencies for any chosen **q** point. The method for the electron-phonon interaction has been well explained in our previous works[6,18,19] and will not be repeated here. We only mention that the density functional theory ensures a reliable framework for implementing from first principles the Migdal-Eliashberg approach[6,13,18–21] for calculating the superconducting properties of materials.

III. RESULTS

A. Structural and electronic properties

YC_2 and LaC_2 materials (see Fig. 1(a)) considered in this study belong to the body-centered tetragonal CaC_2 structure (space group I4/mmm, No. 139), in which Y (La) atom occupies the Wyckoff position 2a (0, 0, 0) and C atoms sit at 4e (0, 0, *z*). Two lattice parameters (*a* and *c*) and one internal parameter (*z*) define the body-centered tetragonal CaC_2 structure. In order to obtain the structural properties of each material, the total energies are calculated for different volumes around the equilibrium one (see Figs. 1(b) and 1(c)). The calculated total energies are fitted to the Murnaghan's equation of state[22] to determine the bulk modulus (*B*) and its pressure derivative (*B*′). The calculated values of lattice parameters (*a* and c), the internal parameter (*z*), the bulk modulus (*B*), and its pressure derivative (*B*′) are presented and compared with available experimental[7,8,11,23–26] and theoretical[10] results in Table I. All sets of parameters for both materials compare very well with their corresponding experimental values.[7,11,24–26] In particular, the calculated lattice parameters (*a* and *c*) and the internal parameter (*z*) are in good accordance with experimental ones,[7,8,11,23–26] with a maximum variation of 0.5%. For the bulk modulus *B* and its pressure derivative *B*′, the agreement with experimental results is very good for LaC_2. Finally, the presently calculated bulk modulus value of 1.06 Mbar for YC_2 shows good agreement with its LDA value of 0.98 Mbar.[10]

The electronic band structures and the total as well as partial eDOS for YC_2 and LaC_2 are illustrated in Figs. 2 and 3, respectively. The overall band profiles for both materials

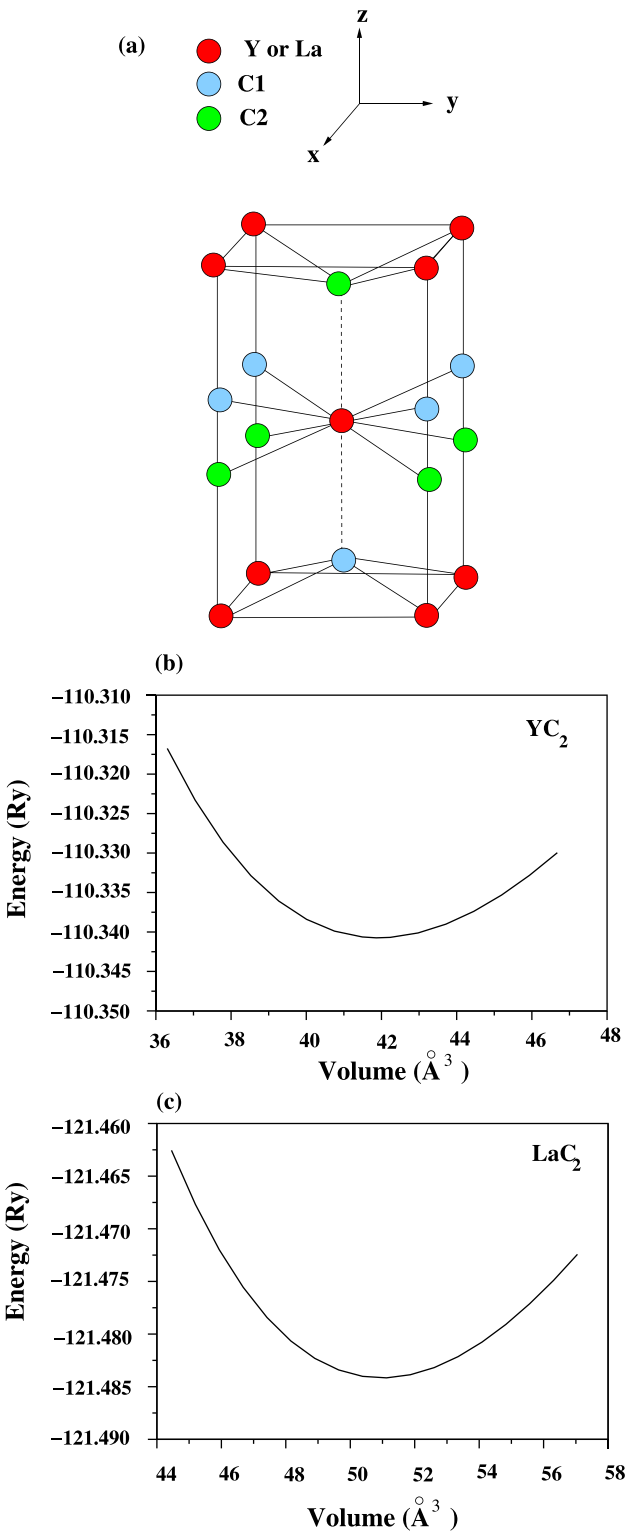

FIG. 1. (a) The CaC_2 structure of YC_2 and LaC_2. (b) Calculated total energies as a function of volume for YC_2. (c) Calculated total energies as a function of volume for LaC_2.

are observed to be in tolerably good accord with previous theoretical calculations.[9,11] The basic physics involved in the discussion of superconductivity involves electronic states near E_F. Such states are very well presented for metallic materials, such as studied here, within the DFT scheme, without any need for any extension of the electron-electron

TABLE I. Static properties of the superconducting YC_2 and LaC_2 and their comparison with available experimental and theoretical results.

Material	*a* (Å)	c (Å)	z	B (Mbar)	B′
YC_2	3.6813	6.1886	0.3947	1.06	4.41
Expt.[8,23,24]	3.6614	6.1725	0.3957		
Expt.[7]	3.6664	6.1400			
LDA[10]				0.98	
LaC_2	3.9376	6.5778	0.4014	0.87	4.48
Expt.[25]	3.9371	6.5792			
Expt.[26]	3.9323	6.5741		0.76	4.61
Expt.[11]	3.9351	6.5746	0.4026		

interaction scheme, as employed in GW calculations. For both materials, the Fermi level is crossed by at least one electronic band which signals the metallic nature of the studied materials. In the case of YC_2, the lowest band is attributed to C 2s and 2p states with lesser contributions coming from Y 4d and 5p states. This band creates a peak at about −7.2 eV in the electronic DOS of YC_2. The second band is mainly dominated by the 2s electrons of C atoms with some contribution coming from the Y 4d orbitals. This band gives rise to a peak at about −4.7 eV in the eDOS of YC_2. Third and fourth bands are due to C 2p states with lesser contributions coming from Y 4d, Y 5s, and C 2s states. These bands generate a peak at about −3.0 eV in the electronic DOS of YC_2. The band close to and crossing the Fermi level arises from Y 4d and C 2p states. Thus, there is a clear hybridization between Y 4d and C 2p states present in the energy region between −2 eV and the Fermi level. As electrons close to the Fermi surface play the main role in the composing of the superconducting state, their nature must be analyzed clearly. The density of states at the Fermi level ($N(E_F)$) for the body-centered tetragonal YC_2 amounts to be 0.78 States/eV which is in excellent agreement with the value of $N(E_F)$ at 0.77 States/eV calculated by Shein and Ivanovskii.[9] In this material, the contribution to $N(E_F)$ from the 4d states and the C 2p states are approximately 55% and 42%, respectively. This observation indicates that the chemical and physical properties of YC_2 correspond to the Y 4d and C 2p bands. Above the Fermi level, the conduction bands of Y 4d and C 2p orbitals with some mixing from other electronic states of Y and C atoms. Generally, the bonding in the body-centered tetragonal YC_2 includes the mixture of metallic, ionic, and covalent. The metallic nature of this material can be related to the partially filled Y 4d bands. The ionic bonding in YC_2 is due to a charge transfer from the Y atom to more electronegative C atom upon the carbide formation. Finally, the covalent bonding in this material is formed by hybridization of the Y 4d and C 2p states, which can be seen clearly from the partial eDOS. The bond between C1 and C2 atoms has also a covalent character.

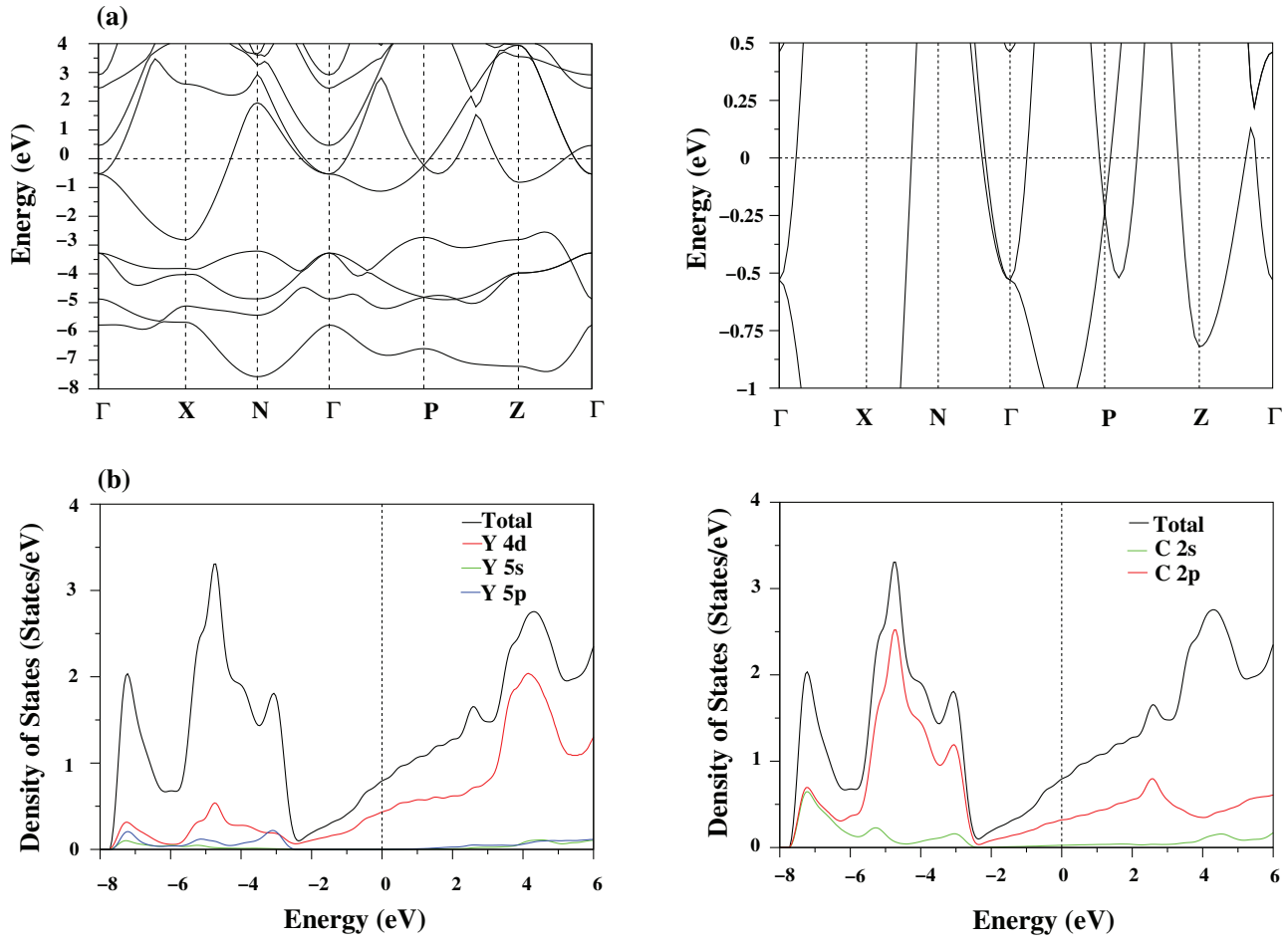

FIG. 2. (a) The electronic band structure for YC_2 along selected symmetry lines in the body-centered tetragonal Brillouin zone. The zero energy represents the Fermi level. (b) The total and partial eDOS curves.

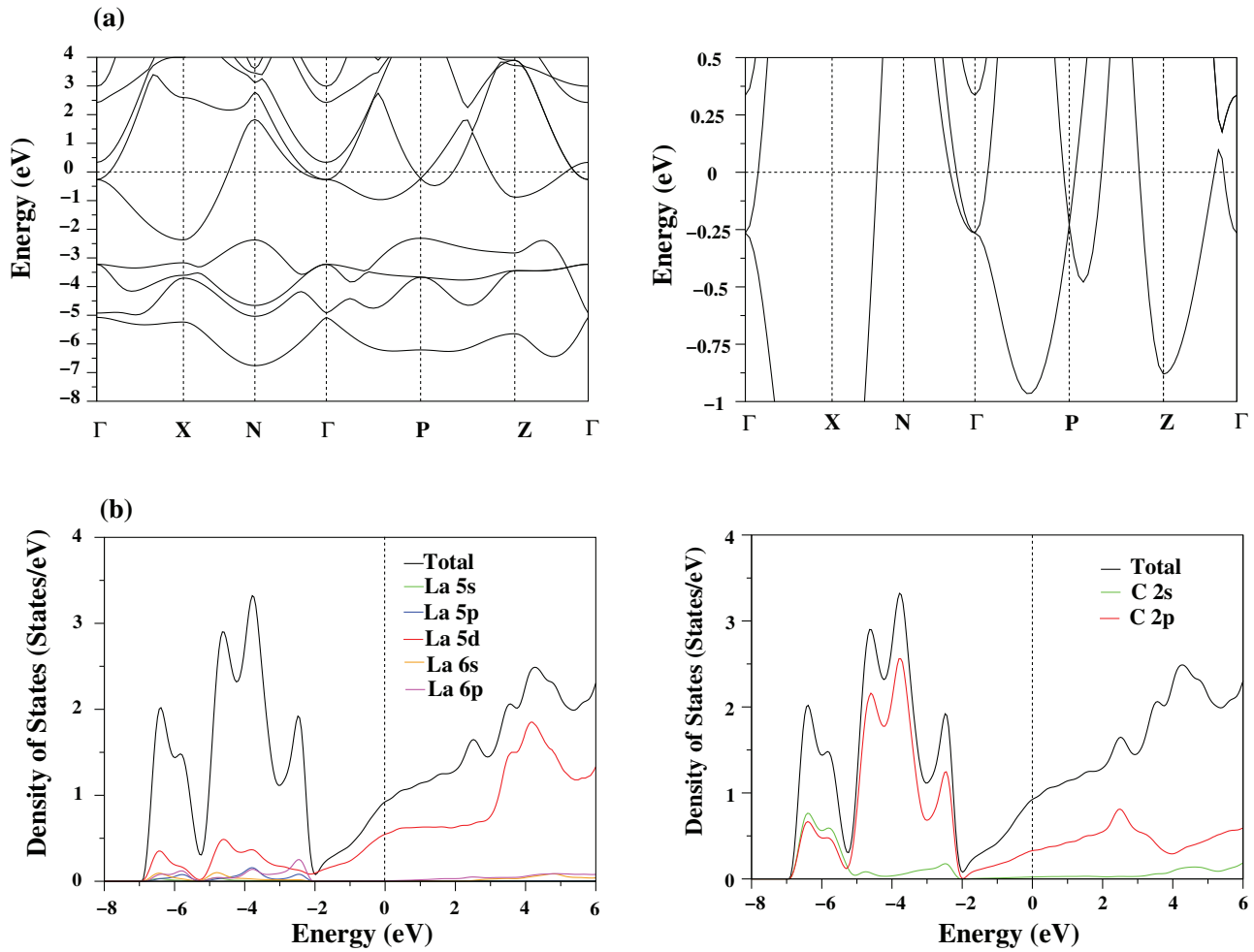

FIG. 3. (a) The electronic band structure for LaC_2. The zero energy represents the Fermi level. (b) The total and partial eDOS curves.

The orbital examination of the eDOS for LaC_2 indicates that mainly La 5d and C 2p states are contributing to the total value of DOS at the Fermi level. The contributions of La 5d and C 2p states are approximately 61% and 38%, respectively. A small amount of C 2s states are mixed with these states. For this material, the value of $N(E_F)$ is found to be 0.86 States/eV. Peaks in the eDOS for LaC_2 have similar structures to the corresponding peaks in the eDOS of YC_2, with Y 4d and Y 5p states replaced with La 5d and La 6p states, respectively.

Despite the general overall similarity of the band structure and eDOS for YC_2 and LaC_2, there are some notable differences near the Fermi energy, as can be inspected from the right-hand panels in Figs. 2 and 3. The depth of the electron pocket at the Γ point is considerably larger in YC_2. We also find that the depth of the electron pocket at the *Z* symmetry point is similar for the two materials, and is larger than the depth of the pocket at Γ. This is in contrast to the TB-LMTO band structure presented by Babizhetskyy *et al.*[11] who find that the pocket at *Z* does not lie below the Fermi energy for LaC_2.

B. Phonons and superconductivity

Fig. 4 shows the phonon dispersion relations along some symmetry directions and the phonon (vibrational) density of states (vDOS) of YC_2. Interestingly, there are three distinct groups of phonon branches, separated from each other by large frequency gaps. In particular, there is a large gap of 4.1 THz between the highest lying acoustic branch and the lowest lying optical branch, and the highest optical branch lies at least 32.7 THz above the rest of the optical branches. The DOS splits into three frequency regimes: 0–5.2 THz, 9.3–13.7 THz, and 46.4–48.9 THz. The Y-related vibrations contribute predominantly to acoustic phonon branches in the low frequency region (LFR) from 0 to 5.2 THz. C atoms also make considerable contribution to this region. Thus, in the whole range 0–5.2 THz a considerable Y-C hybridization can be seen. The Y-related vibrations make a much smaller contribution to the intermediate frequency region (IFR) between 9.3 and 13.7 THz. In this region, the DOS features are mainly characterized by the vibrations of C atoms due to the light mass of C atom. The phonon dispersion curves and DOS of LaC_2 (see Fig. 5) are very similar to those obtained for YC_2. The acoustic phonon modes disperse up to 3.8 THz, five optical phonon modes generate an intermediate frequency region between 7.8 and 11.6 THz, and the highest optic phonon mode disperses from 47.1 to 49.2 THz.

It is interesting to note that the range of the frequency spectrum for the highest phonon branch is very similar for the two materials. The third region from 46.4 to 48.9 THz in

YC_2 and from 47.1 to 49.2 THz in LaC_2 is totally dominated by the vibrations of C atoms. The highest phonon branch in this region has almost pure C1–C2 bond-stretching characteristics, confirming the picture of strongly bonded C dimer in the body-centered tetragonal crystal structure for YC_2 and LaC_2. It is also the frequency of this branch is higher than the corresponding frequency in diamond, graphite, and graphene. This is consistent with the observation that our computed C-C bond length in YC_2 and LaC_2 ($\sim$1.30 Å) is noticeably shorter than the nearest neighbour bond lengths in diamond (1.54 Å), graphite and graphene ($\sim$1.42 Å). This observation indicates that the C1–C2 bond in YC_2 and LaC_2 is more strongly bonded than the carbon bonds in diamond, graphite, and graphene. It is known that Carbon-Carbon bonds lengths range between 1.20 and 1.54 Å depending on the chemical nature of their bonding. Our computed C-C distance in YC_2 and LaC_2 is intermediate to the triple- and double-bond Carbon radii, and in fact is much closer to the double-bond covalent Carbon radii.[27] The dispersive nature of the highest optical phonon branch suggests that there is significant interaction between C1-C2 bonds of neighbouring unit cells along and across the *c*-axis.

Group theoretical treatment of zone-centre phonons in the body-centered tetragonal CaC_2 structure (which YC_2 and LaC_2 assume) with space group I4/mmm yields the following irreducible representations:

$$\Gamma = E_u + A_{2u} + E_g + A_{1g},$$

with two infrared active modes of the species E_u and A_{2u}, and two Raman active modes of the species E_g and A_{1g}. The frequencies of the zone-centre optical phonon modes for both materials are presented in Table II. As the first atom is changed from Y to La, the frequencies of E_u, A_{2u}, and E_g decrease significantly, while that of A_{1g} mode increases only slightly. The frequency decrease of the phonon modes E_{1u},

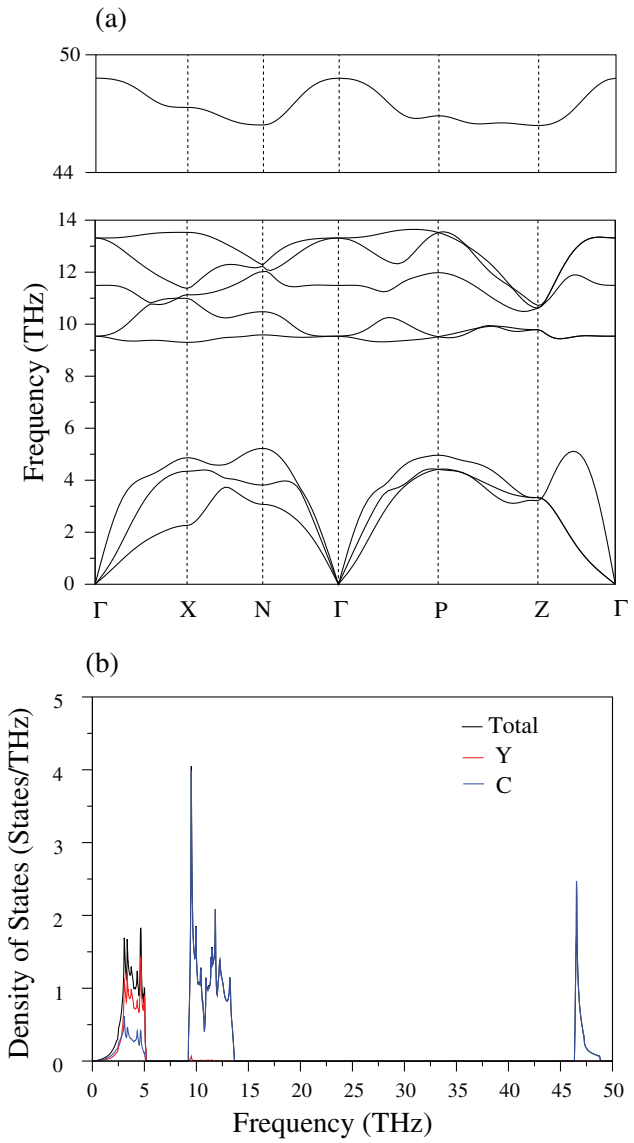

FIG. 4. (a) The phonon dispersion relations for YC_2 along some symmetry directions in the body-centered tetragonal Brillouin zone. (b) The total and partial vDOS curves.

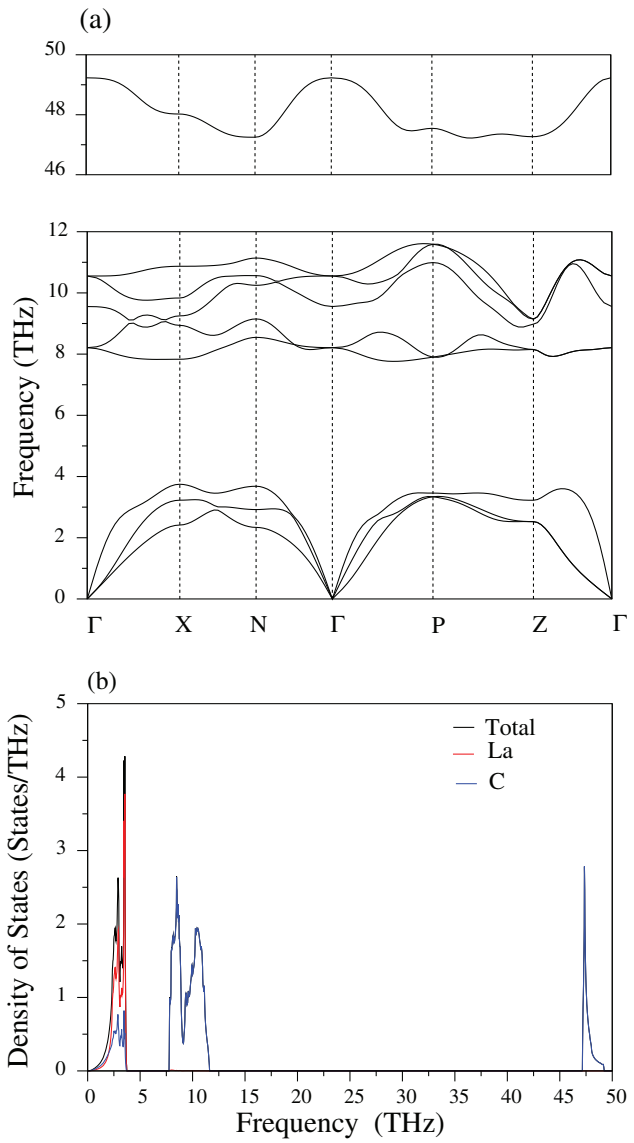

FIG. 5. (a) The phonon dispersion relations for LaC_2 along some symmetry directions in the body-centered tetragonal Brillouin zone. (b) The total and partial vDOS curves.

TABLE II. Calculated zone-centre phonon modes (in THz) for YC_2 and LaC_2.

Material	E_u	A_{2u}	E_g	A_{1g}
YC_2	9.54	11.49	13.32	48.81
LaC_2	8.21	9.56	10.55	49.23

A_{2u}, and E_{2g} can be related to the heavier mass of La atom as compared to that of Y atom and the larger volume of LaC_2 as compared to that of YC_2. The slightly larger frequency of the phonon mode A_{1g} for LaC_2 can related to the slightly shorter C1-C2 bond length ($d^{LaC_2}_{C1-C2} = 1.29$ Å) in LaC_2 as compared to that ($d^{YC_2}_{C1-C2} = 1.29$ Å) in YC_2. The eigendisplacements of the zone-centre phonon modes for YC_2 are shown in Fig. 6. The infrared active modes E_u and A_{2u} are characterized by the opposing vibrations of Y and C atoms along the [010] and [001] directions, respectively. The Raman active modes E_g and A_{1g} come from the opposing motion of the C1 and C2 atoms along the [010] and [001] directions, respectively. The zone-centre phonon modes in LaC_2 have similar atomic displacement patterns to their counterparts in YC_2.

The main objective of this study is to analysis the relative strengths of the electron-phonon interaction in YC_2 and LaC_2 in order to investigate the origin of superconductivity in these materials. Thus, we have presented the calculated Eliashberg spectral function ($\alpha^2F(\omega)$) for YC_2 and LaC_2 in Fig. 7. This function, similar to the phonon density of states, shows sharp features in each of the three frequency regions (LFR, IFR, and HFR—high frequency region). With $\alpha^2F(\omega)$ determined, we can calculate the average electron-phonon coupling parameter λ, which provides a good measure of the overall strength of the electron-phonon interaction, using

$$\lambda = 2\int \frac{\alpha^2F(\omega)}{\omega} d\omega. \quad (1)$$

Using this equation, λ is computed to be 0.55 for YC_2 and 0.54 for LaC_2, which authenticates that the electron-phonon interaction in both these materials is not strong. We further analyze the electron-phonon coupling parameter λ by writing

$$\lambda = \lambda_{LFR} + \lambda_{IFR} + \lambda_{HFR},$$

where

$$\lambda_{region} = \int_{\omega_{min}(region)}^{\omega_{max}(region)} \lambda(\omega) d\omega.$$

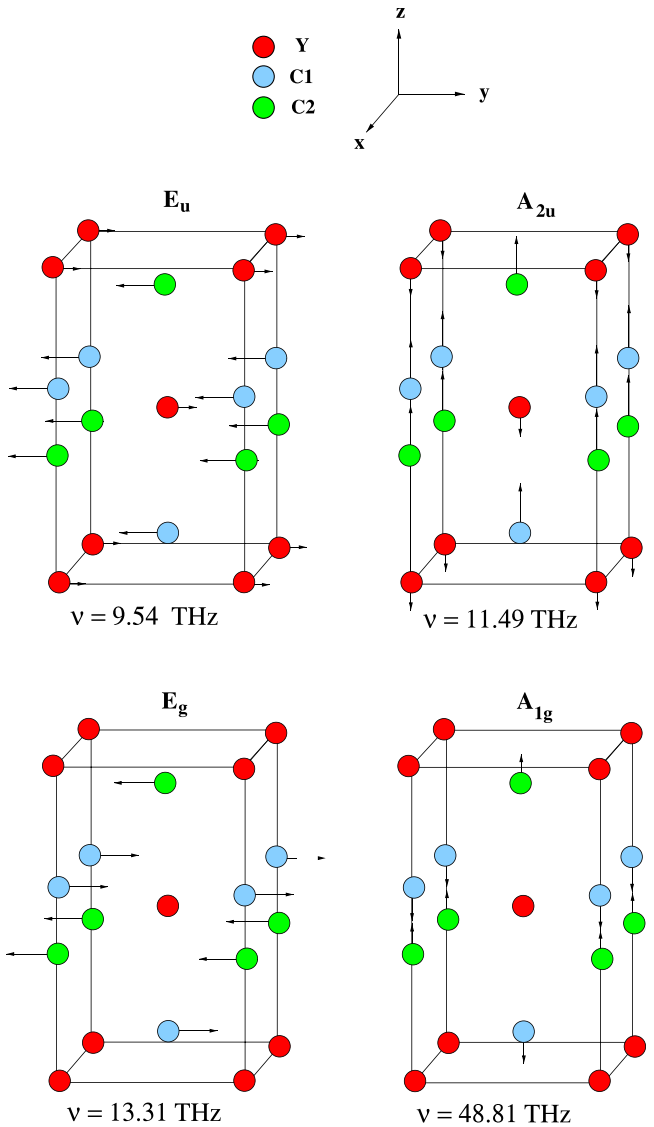

FIG. 6. Eigen atomic displacement patterns for the zone-centre optical phonon modes in the body-centered tetragonal YC_2.

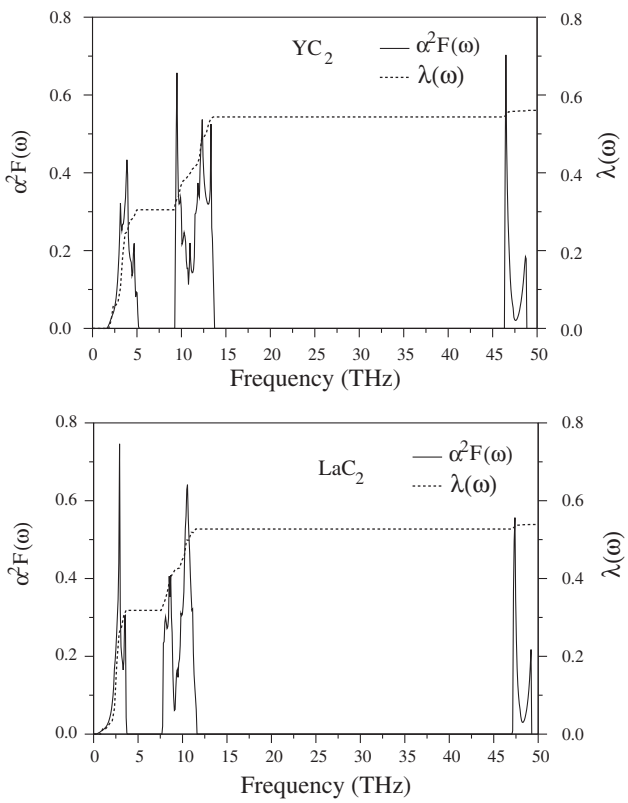

FIG. 7. The calculated Eliashberg spectral function $\alpha^2F(\omega)$ and the integrated electron phonon coupling constant $\lambda(\omega)$ for YC_2 and LaC_2.

The computed values of the electron-phonon interaction parameter in LFR, IFR, and HFR, viz., λ_{LFR}, λ_{IFR}, and λ_{HFR} for YC_2 (LaC_2) are 0.308 (0.318), 0.224 (0.209), and 0.028 (0.011), respectively. The contribution of LFR, IFR, and HFR phonons to λ for YC_2 (LaC_2) is about 55% (59%), 40% (39%), and 5% (2%), respectively. These results indicate that the largest contribution to λ comes from the acoustic phonon modes for both materials. Figs. 4 and 5 clearly show that the acoustic phonon modes are mainly dominated by the coupled motion of Y (La) and C atoms with maximum contribution coming from Y (La) atoms.

From Figs. 2 and 3, we note that the d electrons of Y (or La) atoms make the largest contribution to the eDOS at the Fermi energy. We can therefore conclude that for both materials the largest contribution to λ comes from the Y (La) atoms from strong coupling of their d electrons with their acoustic vibrations (in the LFR range). The intermediate-frequency phonon modes also make considerable contribution to λ. This result is also expected because C atomic vibrations play important role in this frequency region and C p orbitals make significant contribution to the electronic density of states $N(E_F)$. Finally, the smallest contribution to λ comes from the highest optical phonon frequency for both materials. This is unsurprising in view of the factor $1/\omega$ in the denominator of Eq. (1).

According to the Allen-Dynes modification of the McMillian formula[28,29]

$$T_C = \frac{\omega_{\ln}}{1.2}\exp\left(-\frac{1.04(1+\lambda)}{\lambda-\mu^*(1+0.62\lambda)}\right), \quad (2)$$

two main factors effect the superconductor transition temperature (T_C): the strength of electron-phonon coupling parameter λ and the logarithmic average phonon frequency ω_{ln} expressed as

$$\omega_{ln} = \exp\left(\frac{2}{\lambda}\int_o^\infty ln(\omega)\frac{d\omega}{\omega}\right). \quad (3)$$

Using the above equation, the value of ω_{ln} is found to be 300.12 K for YC_2 and 228.26 K for LaC_2. It is well known that the Coulomb pseudo-potential μ^* takes values between 0.10 and 0.16.[28,29] In our calculations, we have decided to use the average of these limiting values, i.e., $\mu = 0.13$. Inserting the computed values of λ and ω_{ln}, and the choice $\mu^* = 0.13$ into the simplified Allen-Dynes formula, the value of T_C is found to be 3.81 K for YC_2 and 2.44 for LaC_2.

The electronic specific heat coefficient γ is calculated from

$$\gamma = \frac{1}{3}\pi^2 k_B^2 N(E_F)(1+\lambda). \quad (4)$$

We have compared our superconducting parameters of YC_2 and LaC_2 with their corresponding experimental values in Table III. The calculated values of λ, T_C, and γ for both materials compare very well with their corresponding experimental values. Both experimental and our theoretical calculations show that T_C for YC_2 is larger than that for LaC_2.

TABLE III. The calculated superconducting state parameters for YC_2 and LaC_2 and their comparison with the corresponding experimental results.

Material	$N(E_F)$ (States/eV)	λ	ω_{ln} (K)	T_C (K)	$\gamma\left(\frac{mJ}{mol\,K^2}\right)$
YC_2	0.78	0.56	300.12	3.81	2.86
Expt.[8]				3.88	
Expt.[7]		0.55		4.02	2.79
TB-LMTO-ASA[7]	0.68				
GGA[9]	0.77				
LaC_2	0.86	0.54	228.26	2.44	3.11
Expt.[12]				1.60	
Expt.[11]		0.49			2.41

This can be related to the slightly larger values of λ and ω_{ln} for YC_2 as compared to those for LaC_2.

We now make a comparison of superconductivity between YC_2 and Y_2C_3 by examining their electronic and phonon structures. The latter is superconductor[30] with a high T_c of 18 K. The superconducting parameters of these superconductors are compared in Table IV. Three main factors effect T_C for the BCS-type superconductors: the electronic DOS at the Fermi level $N(E_F)$, the logarithmic average phonon frequency ω_{ln} (or the averaged square of the phonon frequency $\langle\omega^2\rangle$), and the strength of electron-phonon coupling parameter λ. The value of $N(E_F)$ for YC_2 is more than two times lower than that for Y_2C_3. This change effects the value of λ because it is directly connected to the change in $N(E_F)$ due to the McMillan-Hopfield expression $\lambda = \frac{N(E_F)\langle I^2\rangle}{M\langle\omega^2\rangle}$, where $\langle I^2\rangle$ is the averaged square of the electron-phonon matrix element, $\langle\omega^2\rangle$ is the averaged square of the phonon frequency, and M is the mass involved. Thus, λ of YC_2 becomes much smaller than that of Y_2C_3. Although the value of ω_{ln} for Y_2C_3 is smaller that the corresponding value for YC_2, soft phonon frequencies make a positive contribution to the electron-phonon coupling parameter due to the McMillan-Hopfield expression. As a result, the T_c value for YC_2 is much smaller than that for Y_2C_3 due difference in their density of states at the Fermi level and electron-phonon coupling parameter. A similar observation can be made for LaC_2 and La_2C_3 superconductor[33] with a high T_c of 10.9 K.

C. Summary

In this work, we have studied the structural, electronic, phonon, and electron-phonon properties of YC_2 and LaC_2 by using the generalized gradient approximation of the density functional theory and the planewave *ab initio* pseudopotential method.

TABLE IV. Comparison of superconducting state parameters for YC_2 and Y_2C_3. LPAPW stands for generalized potential linearized augmented plane wave.

Material	$N(E_F)$ (States/eV)	λ	ω_{ln} (K)	T_C (K)
YC_2 (GGA)	0.78	0.56	300.12	3.81
Y_2C_3 (LPAPW)[31]	1.88	~1	251.82	
Y_2C_3 (GGA)[32]	1.56	1.35		
Y_2C_3 (Expt.)[30]				18

Analysis of the electronic properties shows that the bonding in both materials can be classified as a mixture of metallic, ionic, and covalent contributions. These contributions arise, respectively, from the partially filled Y (La) d bands, due to a substantial charge transfer from the Y (La) atoms to the more electronegative C atoms, and by the hybridization of the C p and Y (La) d states. The density of states at the Fermi energy is dominated by the hybridization of Y d (La d) and C p states.

No unstable phonon modes appear for the phonon dispersion curves of both materials, confirming that the both materials are dynamically stable in the body-centered tetragonal CaC_2 structure. The phonon DOS for both materials can be divided into three clearly distinct regions: low frequency, intermediate frequency, and high frequency regions. The low frequency region accommodates the acoustic phonon branches which are characterized by in-phase coupled motions of Y (La) and two C atoms.

Analysis of the Eliashberg spectral function $\alpha^2F(\omega)$ reveals the importance of the coupled in-phase motions of Y (La) and two C atoms which makes the largest contribution to the average electron-phonon coupling parameter λ due to the strong hybridization of Y d (La d) and C p states close to the Fermi energy. By integrating the Eliashberg spectral function, the average electron-phonon coupling parameter λ is found to be 0.55 for YC_2 and 0.54 for LaC_2, indicating that these are weak-coupling BCS superconductors. Using the Allen-Dynes modified McMillian equation with the screened Coulomb pseudopotential parameter $\mu^* = 0.13$, the superconducting temperature is found to be 3.81 K for YC_2 and 2.44 K for LaC_2. These values are in good agreement with their experimental values of 4.02 K for YC_2 and 1.61 K for LaC_2. The experimental and theoretical T_C values of YC_2 are slightly larger than the corresponding values of LaC_2, which can be linked to the slightly larger values of λ and ω_{ln} for YC_2 as compared to those for LaC_2.

[1]M. Gupta and A. J. Freeman, Phys. Rev. B **14**, 5205 (1976).
[2]P. Blaha and K. Schwarz, Int. J. Quantum Chem. **23**, 1535 (1983).
[3]A. F. Guillermet, J. Häglund, and G. Grimvall, Phys. Rev. B **45**, 11557 (1992).
[4]H. R. Zeller, Phys. Rev. B **5**, 1813 (1972).
[5]W. Weber, Phys. Rev. B **8**, 5082 (1973).
[6]H. M. Tütüncü, S. Bağcı, G. P. Srivastava, and A. Akbulut, J. Phys.: Condens. Matter **24**, 455704 (2012).
[7]Th. Gülden, R. W. Henn, O. Jepsen, R. K. Kremer, W. Schnelle, A. Simon, and C. Felser, Phys. Rev. B **56**, 9021 (1997).
[8]A. L. Giorgi, E. G. Szklarz, M. C. Krupka, T. C. Wallace, and N. H. Krikorian, J. Less-Common Met. **14**, 247 (1968).
[9]I. R. Shein and A. L. Ivanovskii, Solid State Commun. **131**, 223 (2004).
[10]X. Gao, Y. Jiang, R. Zhou, and J. Feng, J. Alloys Compd. **587**, 819 (2014).
[11]V. Babizhetskyy, O. Jepsen, R. K. Kremer, A. Simon, B. Ouladdiaf, and A. Stolovits, J. Phys.: Condens. Matter **26**, 025701 (2014).
[12]R. W. Green, E. O. Thorland, J. Croat, and S. Legvold, J. Appl. Phys. **40**, 3161 (1969).
[13]P. Giannozzi, S. Baroni, N. Bonini, M. Calandra, R. Car, C. Cavazzoni, D. Ceresoli, G. L. Chiarotti, M. Cococcioni, I. Dabo, A. D. Corso, S. de Gironcoli, S. Fabris, G. Fratesi, R. Gebauer, U. Gerstmann, C. Gougoussis, A. Kokalj, M. Lazzeri, L. Martin-Samos, N. Marzari, F. Mauri, R. Mazzarello, S. Paolini, A. Pasquarello, L. Paulatto, C. Sbraccia, S. Scandolo, G. Sclauzero, A. P. Seitsonen, A. Smogunov, P. Umari, and R. M. Wentzcovitch, J. Phys.: Condens. Matter **21**, 395502 (2009).
[14]J. P. Perdew, K. Burke, and M. Ernzerhof, Phys. Rev. Lett. **77**, 3865 (1996).
[15]D. Vanderbilt, Phys. Rev. B **41**, 7892 (1990).
[16]W. Kohn and L. J. Sham, Phys. Rev. **140**, A1133 (1965).
[17]H. J. Monkhorst and J. D. Pack, Phys. Rev. B **13**, 5188 (1976).
[18]S. Bağcı, S. Duman, H. M. Tütüncü, and G. P. Srivastava, Phys. Rev. B **78**, 174504 (2008).
[19]S. Bağcı, H. M. Tütüncü, S. Duman, and G. P. Srivastava, Phys. Rev. B **81**, 144507 (2010).
[20]A. B. Migdal, Sov. Phys. JETP **34**, 1438 (1958).
[21]G. M. Eliashberg, Sov. Phys. JETP **11**, 696 (1960).
[22]F. D. Murnaghan, Proc. Natl. Acad. Sci. U. S. A. **30**, 244 (1944).
[23]M. Atoji, J. Chem. Phys. **35**, 1950 (1961).
[24]D. W. Jones, I. J. McColm, R. Steadman, and J. Yerkess, J. Solid State Chem. **53**, 376 (1984).
[25]D. W. Jones, I. J. McColm, and J. Yerkess, J. Solid State Chem. **92**, 301 (1991).
[26]X. Wang, I. Loa, K. Syassen, R. K. Kremer, A. Simon, M. Hanfland, and K. Ahn, Phys. Rev. B **72**, 064520 (2005).
[27]G. Burns, *Solid State Physics* (Academic Press, Inc., London, 1985).
[28]P. B. Allen, Phys. Rev. B **6**, 2577 (1972).
[29]P. B. Allen and R. C. Dynes, Phys. Rev. B **12**, 905 (1975).
[30]G. Amano, S. Akutagawa, T. Muranaka, Y. Zenitani, and J. Akimitsu, J. Phys. Soc. Jpn. **73**, 530 (2004).
[31]D. J. Singh and I. I. Mazin, Phys. Rev. B **70**, 052504 (2004).
[32]C. Yu, J. Liu, H. Lu, P. Li, R. Fan, and J. Xiao, Solid State Commun. **142**, 536 (2007).
[33]S. Kuroiwa, Y. Saura, J. Akimitsu, M. Hiraishi, M. Miyazaki, K. H. Satoh, S. Takeshita, and R. Kadono, Phys. Rev. Lett. **100**, 097002 (2008).